Signal, Image and Video Processing (2019) 13:1183–1190
https://doi.org/10.1007/s11760-019-01462-z

ORIGINAL PAPER

Force classification using surface electromyography from various object lengths and wrist postures

Sirinapa Jitaree[1] · **Pornchai Phukpattaranont**[1]

Received: 2 August 2018 / Revised: 23 January 2019 / Accepted: 16 March 2019 / Published online: 23 March 2019

Abstract
Pattern recognition using myoelectric control of upper-limb prosthetic devices is essential to restore control of several degrees of freedom. Although much development has been relevant, the prediction of force level in finger movements is scanty. In this study, we propose the surface electromyography (sEMG) to predict the force level of the thumb-index pinch. Ten non-amputee subjects are asked to do five force levels with three different wrist positions and five object lengths. The sEMG data are recorded from three muscle regions (12 channels) of the right forearm. Twelve traditional time-domain features are extracted from collected sEMG signal. The sequential forward floating selection (SFFS) method is investigated to find the optimal set of muscles and features for force prediction. Performances from seven linear and nonlinear classifiers are compared. The results show that *k*-nearest neighbor and neural network outperform other classifiers with the accuracy of about 99% and 97%, respectively. The accuracy from the set of muscle groups and features selected by SFFS method is slightly better than that from the set of baseline (all of channels and features). The frequently selected muscles are from the hand region. However, the combination of lower and upper muscles also performs well, which is useful for the prosthetic design in a hand and wrist disarticulation amputee and a transradial amputee in the future.

Keywords EMG · Prosthetic devices · SFFS · *K*-nearest neighbor · Neural network · Proportional myoelectric control

1 Introduction

The loss of upper-limb function is a disability that limits the capabilities and interactions in the daily life of a person [1]. To improve the quality of life of amputees, the prosthetic devices, which are controlled by the pattern recognition system based on surface electromyography (sEMG) signals from the residual muscles, the arm or the shoulder, are developed [2–4]. However, in the real environment, a change in force level or limb position can deteriorate their performance [5–9].

Kamavuako et al. [5] studied the correlation between force profiles and single-channel intramuscular EMG (iEMG). The correlation coefficient between the iEMG and force was approximately 0.9, which was quite similar to that from the sEMG and force. He et al. [6] proposed the novel features based on discrete Fourier transform to classify 9 grasp and wrist motions under 3 muscle contraction levels (20, 50, and 80% of maximal voluntary contraction) with linear discriminant analysis (LDA). Results showed that the proposed features provided better classification accuracy compared to that from the traditional time-domain features because of their robust property, which can be against varying contraction levels. In [7], the popular time-domain features from sEMG, such as root mean square (RMS), mean absolute value (MAV), were used as the inputs of the time-delayed artificial neural network to predict forearm muscle forces during the extension and flexion wrist movements in real time.

In [8], a novel set of features based on Fourier transform relations, the Parseval's theorem, and power spectrum moments, which was able to be against force variation, was developed. It was used to classify 6 motions including different grip and finger movements under 3 force levels (low, moderate, high). Four classifiers including LDA, Naïve Bayes (NB), random forest, and *k*-nearest neighbor

✉ Pornchai Phukpattaranont
pornchai.p@psu.ac.th

Sirinapa Jitaree
s.jitaree002@gmail.com

[1] Faculty of Engineering, Department of Electrical Engineering, Prince of Songkla University, Hat Yai, Songkhla 90112, Thailand

(KNN) were compared. Results showed that the proposed set of features could improve the classification performance (6–8%) in comparison with other methods of feature extraction and LDA gave the best performance compared to other classifiers.

Celadon et al. [9] estimated force profiles and force levels from individual finger movements (flexion and extension) using high-density sEMG. RMS was used as the feature. Three methods including LDA, common spatial patterns proportional estimator (CSP-PE), and thresholding algorithm were evaluated and compared. Results showed that the performance from the CSP-PE was the best when the number of electrodes was less than 24. However, for higher resolution of the recording, the performance from CSP-PE was comparable to that from LDA.

Effective features are essential in pattern recognition for myoelectric control. Dimensionality reduction is usually applied when the number of channels used to record sEMG signals is large to reduce redundancy and increase the relevance of the features. Adewuyi et al. [10] studied 5 sEMG feature sets for classifying 4 hand motions in different wrist positions from 16 non-amputees and 4 partial-hand amputees. Results showed that the feature subset from LDA combined with a feature selection algorithm based on the sequential forward searching (SFS) method gave the lowest classification error. However, the main drawback of SFS method is the nesting effect [11], i.e., inability to remove the added feature.

In this paper, the sequential forward floating selection (SFFS), which is a suboptimal search strategy to solve the nesting effect [12], is applied to select the optimal feature subset for classification of 5 force levels. Twelve channels of sEMG signals from the muscles in 3 upper-limb regions including the region of hand (RH), the region of the lower forearm (RLF) and region of the upper forearm (RUF), were recorded from thumb-index pinch with 3 wrist postures, 5 length objects, and 5 force levels. The classification errors from the muscles in RH, RLF, and RUF would be evaluated and compared so that the muscles can be appropriately chosen and used.

2 Materials and methods

2.1 EMG data acquisition

In this study, twelve channels of sEMG signals were recorded from 3 regions on the right arm including RH, RLF, and RUF as shown in Fig. 1. The list of related muscles in each region is shown in Table 1. The muscles in RH, RLF, and RUF are shown in Figs. 2, 3 and 4, respectively. Details of muscles in each region are as follows.

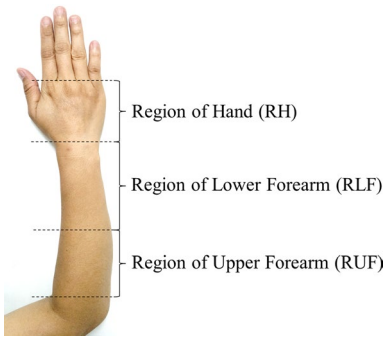

Fig. 1 Three regions of the forearm used in sEMG data acquisition

Table 1 List of related muscles in each region

Regions	Channels	Muscles
RH	3	AP, APB, FDI (c1–c3)
RLF	2	FPL, EPL (c4–c5)
RUF	7	ECU, EDC, EDM, ECRL, ECRB, BR, FCR, PL, FDS, FCU, FDP (c6–c12)

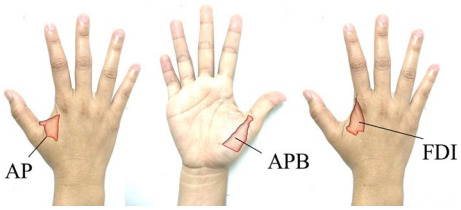

Fig. 2 Three muscles in RH including the AP (left), the APB (Middle), and the FDI (right)

Fig. 3 Two muscles in RLF including the FPL (left) and the EPL (right)

RH The sEMG data from 3 muscles in RH consisting of the adductor pollicis (AP), the abductor pollicis brevis (APB), and the first dorsal interosseous (FDI) were collected from bipolar Ag/AgCl electrodes (EL254S, BIOPAC) at an inter-electrode distance 10 mm.

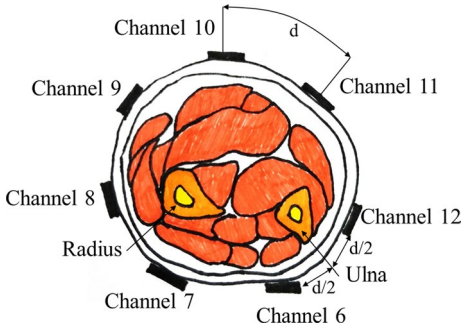

Fig. 4 Cross section of the RUF indicating approximate electrode locations

RLF The sEMG data from 2 muscles in RLF including the flexor pollicis longus (FPL) and the extensor pollicis longus (EPL) were recorded using bipolar Ag/AgCl electrodes (H124SG, Kendel ARBO) at an inter-electrode distance 20 mm.
RUF Seven pairs of electrodes were placed in RUF without specific muscle positions at approximately one-third of the forearm length from the head of the ulna. The type and configuration of electrodes used were the same as in RLF. The distances between adjacent electrodes (d) were approximately equal. The first pair of the electrode was placed at a distance of $d/2$ from the ulnar.

All sEMG data were acquired by a commercial measurement system (MP150, BIOPAC system). A band-pass filter of 10 Hz to 500 Hz and an amplifier gain of 1000 times were set. The sEMG data were sampled at a rate of 1000 Hz. Force data were measured using a force sensor (KISTLER 9017B) and recorded synchronously with sEMG data. Ten healthy subjects (6 males and 4 females) joined the experiment. Mean and standard deviation of subjects' age were 29.9 ± 6.9 years. They were asked to maintain 5 object lengths (i.e., 45, 60, 75, 90, and 105 mm) with thumb-index pinch at 3 wrist postures (i.e., flexion, neutral, and extension). For each subject, a total of 225 datasets were collected (3 wrist postures $\times$ 5 object lengths $\times$ 5 force levels $\times$ 3 trials). More details about the postures and experiments could be found in [13]. Example of sEMG signals at 5 force levels from the AP muscle (c1) acquired with the object length 75 mm and the wrist extension is shown in Fig. 5.

2.2 Methods

Figure 6 shows the proposed method for force classification from thumb-index pinch using sEMG consisting of 3 stages, i.e., (1) Preprocessing, (2) Feature selection, (3) Classification. The details of each analytical stage are as follows.

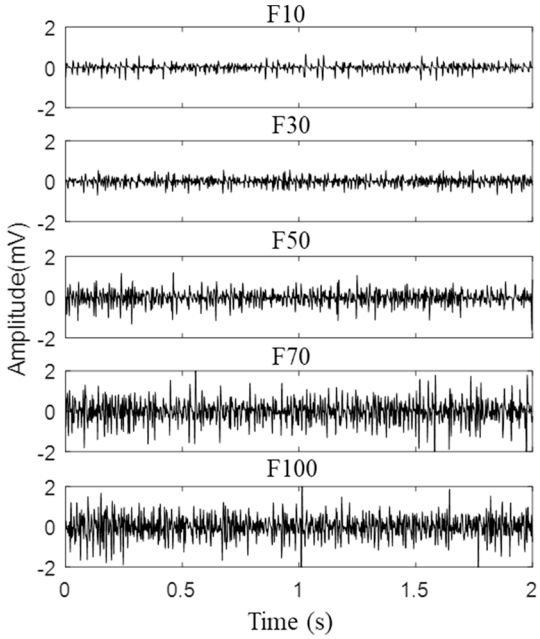

Fig. 5 Example of the sEMG signals from the AP muscle (c1) of wrist extension posture and object length 75 mm with each force level in each row, respectively

2.2.1 Preprocessing

There are four main steps in preprocessing. The first step is noise removal using a notch filter. Then, the filtered sEMG with the length of 2s is segmented using the 256 ms analysis window with 50% overlap [14]. As a result, fourteen sEMG segments are obtained for each sEMG channel. Next, in the feature calculation step, twelve frequently used time-domain features described in Table 2 are determined from each sEMG segment. In total, the feature vector with dimension 144 (12 features per channel $\times$ 12 channels) is obtained for each force level of each subject. Finally, the values from each channel and feature pair in all force levels are normalized so that their values are in the range of -1 to 1.

2.2.2 Feature selection

To reduce the computational complexity and processing time, a smaller dimension of features can be obtained by feature selection techniques. Given a set of feature Y, the method will select a smaller subset of feature X that performs the best performance for the criterion function, $J(X)$. Typically, a subset $X \subseteq Y$ can be found by

$$J(Y) = \max_{X \subseteq Y, |X| = f} J(X), \tag{1}$$

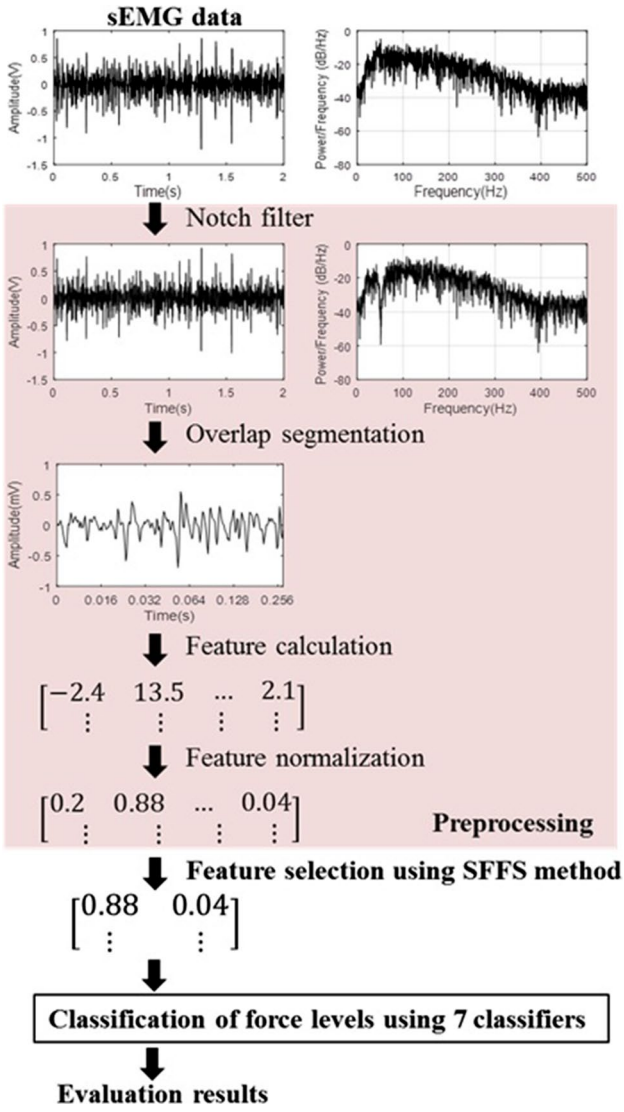

Fig. 6 Method for force classification from the thumb-index pinch using sEMG signals

where f is the desired number of selected features. However, the exhaustive search is exponential and impractical for even moderate values of Y [16]. In this study, the feature selection using the correlation forward selection based on SFFS method is used. The SFFS proposed by Pudil et al. [12] is defined by floating up and down during the search. It starts from the empty set that evaluates all possible single-feature expansions of the current subset.

The SFFS was applied to select the optimal feature subset from each feature vector for force classification. To find the optimum distance for SFFS, six criteria were tested including (1) inter–intra distance (inin), (2) sum of estimated Mahalanobis distances (mahas), (3) minimum of estimated Mahalanobis distances (maham), (4) sum of squared Euclidean distances (eucls), (5) minimum of squared Euclidean distances (euclm), and (6) 1-nearest neighbor. Results show that 1-nearest neighbor can reach the maximum distance at the feature dimension of 10, which is faster than other criteria. Therefore, the feature subset obtained from 1-nearest neighbor is used as the input of classifiers in the next stage.

2.2.3 Classification

In this study, seven classifiers, namely decision tree (DT), LDA, quadratic discriminant analysis (QDA), support vector machine (SVM), KNN, NB, and neural network (NN), were tested and compared. For each subject, the cross-validation was applied for the performance evaluation of each classifier. The tenfold cross-validation was used. In other words, data were divided into ten subsets. In each round, one of them was testing data, while others were training data. In total, ten classification errors were obtained with different subsets of testing data. The performance from each classifier was measured by means and standard deviation of classification errors from ten subjects. Brief descriptions and the parameters used for each classifier are described as follows.

a. DT classifier is based on hierarchy. Its model is constructed in the form of a tree structure including node, branch, and leaf. Nodes are the features, branches are the possible outcome of the test, and leaves are the class labels [17]. In this study, the splitting criterion was defined as purity, and the pruning was not used.
b. LDA classifier is a linear and binary supervised algorithm that considers a probability distribution between two classes to assign the class of unknown data. In a multi-class classification problem, a one versus all approach is applied to this binary classifier. LDA aims to solve the following problem:

$$y = \omega^{\mathrm{T}} x + \omega_0. \tag{2}$$

Vector x is the feature vector. Vectors ω and ω_0 are identified by spreading interclass means and reducing interclass variance [18]. In this study, LDA was computed without regularization. Because of no manually specified internal parameters in this classifier, the trial-and-error approach using cross-validation of training set was applied.
c. QDA produces a quadratic line for separation of two classes based on their Gaussian densities with unequal variances [19]. The purpose is to calculate the decision boundary as denoted in:

$$y = x^{\mathrm{T}} \omega x + \omega^{\mathrm{T}} x + \omega_0. \tag{3}$$

Parameter tuning of QDA in this study was the same as LDA.
d. SVM is a supervised algorithm proposed by Vapnik [20]. The general concept of SVM is to operate a discriminant

Table 2 List of time-domain features used in this study

Feature name	Equation
f1: Difference Absolute Standard Deviation Value (DASDV)	$\mathrm{DASDV} = \sqrt{\frac{1}{N-1}\sum_{n=1}^{N-1}\left(x_{n+1}-x_n\right)^2}$
f2: Log Detector (LOG)	$\mathrm{LOG} = \mathrm{e}^{\frac{1}{N}\sum_{n=1}^{N}\log\left(\lvert x_n\rvert\right)}$
f3: Modified MAV 1 (MAV1)	$\mathrm{MAV1} = \frac{1}{N}\sum_{n=1}^{N} w_n\lvert x_n\rvert$ $w_n = \begin{cases} 1, & \text{if } 0.25N \le n \le 0.75N \\ 0.5, & \text{otherwise} \end{cases}$
f4: Modified MAV 2 (MAV2)	$\mathrm{MAV2} = \frac{1}{N}\sum_{n=1}^{N} w_n\lvert x_n\rvert$ $w_n = \begin{cases} 1, & \text{if } 0.25N \le n \le 0.75N \\ 4n/N, & \text{else if } n < 0.25N \\ 4(n-N)/N, & \text{otherwise} \end{cases}$
f5: Mean Absolute Value (MAV)	$\mathrm{MAV} = \frac{1}{N}\sum_{n=1}^{N}\lvert x_n\rvert$
f6: Maximum Fractal Length (MFL) [15]	$\mathrm{MFL} = \frac{\left\{\left(\sum_{n=1}^{\left[\frac{N-m}{k}\right]}\lvert x(m+nk)-x(m+(n-1).k)\rvert\right)\frac{N-1}{\left[\frac{N-m}{k}\right].k}\right\}}{k}, \quad (m = 1, 2, \ldots, k)$
f7: Root Mean Square (RMS)	$\mathrm{RMS} = \sqrt{\frac{1}{N}\sum_{n=1}^{N} x_n^2}$
f8: Third Temporal Moment (TM3)	$\mathrm{TM3} = \left\lvert\frac{1}{N}\sum_{n=1}^{N} x_n^3\right\rvert$
f9: Forth Temporal Moment (TM4)	$\mathrm{TM4} = \left\lvert\frac{1}{N}\sum_{n=1}^{N} x_n^4\right\rvert$
f10: Fifth Temporal Moment (TM5)	$\mathrm{TM5} = \left\lvert\frac{1}{N}\sum_{n=1}^{N} x_n^5\right\rvert$
f11: Variance (VAR)	$\mathrm{VAR} = \frac{1}{N-1}\sum_{n=1}^{N} x_n^2$
f12: Waveform Length (WL)	$\mathrm{WL} = \sum_{n=1}^{N-1}\lvert x_{n+1}-x_n\rvert$

N denotes the window length, x_n is the nth EMG sample within the current window. In MFL, $k = 128$ and m integers represent time interval and initial time, respectively

hyperplane to separate the classes of data set, especially in nonlinearly separable problems [21]. It aims to find the optimal hyperplane that maximizes the margins between the data set. In this study, the radial basis function was selected as the kernel function because of its success in previous publications [22, 23]. Moreover, in our tests, it outperformed the second-order polynomial kernel and the sigmoid function. The cost parameter was 1.0, and the kernel parameter (γ) was $1/n$ (n is the dimension of the feature vector from SFFS).

e. KNN classifier known as the lazy learning algorithm is efficient and straightforward in machine learning [24]. Its process starts with calculations of distances between testing data and training data. The distance values among the test sample to other samples would be measured by various methods such as Euclidean distance and Minkowski distance. Then, they are sorted in descending order and the majority vote designates the class of testing data among the k largest distances. In this study, the Euclidean distance was used and the number of the nearest neighbors k was optimized based on the leave-one-out error on the dataset.

f. NB classifier is a simple probabilistic classifier based on Bayes rule. It aims to reach the best hypothesis through a given training data set. Bayes theorem provides a way to calculate the probability of a hypothesis based on its prior probability of both the data found and the total data [25]. In this study, the number of bins 49 was used

to find the class based on the maximum posterior probability.

g. NN classifier is a typical nonlinear classifier. In this study, a feed-forward artificial neural network was used. It consisted of one input layer, one hidden layer, and one output layer. The hyperbolic tangent sigmoid function was used in all layers. The features extracted were input to the network. The number of neurons in the input layer was equal to the number of features selected by SFFS. The number of neurons in the hidden layer at 10, 20, and 30 was tested and compared. The one that gave maximum accuracy was selected. The output layer had 5 neurons, which was equal to the number of force levels. Levenberg–Marquardt was applied in this study because it provided fast training on the moderate-sized network for solving pattern recognition problems using the numerical optimization technique. Loss function used in neural network training was mean square error. The maximum error during the training was defined as $0.02/m$, where m is the size of training data.

3 Results

3.1 Feature selection

Figure 7 shows the number of selections in each feature and channel pair accumulated from ten subjects. The f1c1 and f1c4 are the highest frequently selected pairs (5 subjects). On the other hand, while the 3 lowest frequently selected features are f4, f9, and f10 (the number of selections ≤ 5), the 5 lowest frequently selected channels are c5, c8, c9, c10, and c11 (the number of selections ≤ 15). While the most frequently selected features are f1 (DASDV) and f6 (MFL) at approximately 16%, f10 (TM5) is the least frequently chosen feature (1.9%). Two most frequently selected channels are c3 in RH and c12 in RUF, whereas the EPL muscle (c5) in RLF is scanty in selection.

3.2 Classification

Figure 8 shows the classification errors averaged from ten subjects from all feature inputs (dark) compared with those from SFFS feature inputs (gray). The errors from all feature inputs are comparable to those from the SFFS feature inputs in all classifiers except for LDA and SVM. The errors from DT, LDA, QDA, and NB classifiers are higher than 10%. In SVM, the classification error from the SFFS inputs reaches 13%, which is almost 3 times greater than the errors from all feature inputs. The KNN classifier gives the best performance at 0.8% for all feature inputs and 0.2% for SFFS feature inputs. NN classifiers perform better when the number of neurons in the hidden layer increases from 10 to 20 and 30 at the expense of computational complexity. The errors from NN-30 with all and SFFS feature inputs are 2.5% and 3%, respectively. These results indicate that the feature set selected from SFFS can be used as the inputs of KNN and NN classifiers for classification of force levels.

Figure 9 shows the classification errors categorized by 5 muscle regions when the SFFS features are used as the inputs of LDA, KNN, and NN-30. While KNN and NN-30 are used in comparisons because they give high classification performance, LDA is chosen because it is widely used in previous studies of sEMG classification. Results show that the minimum errors are obtained when all muscle regions are used. The errors increase when only some muscle regions are used. For example, in KNN classifier, the error from RLF + RUF (c4–c12) increases to 6.9% compared to that from RH + RLF + RUF (c1–c12), which is only 0.2%.

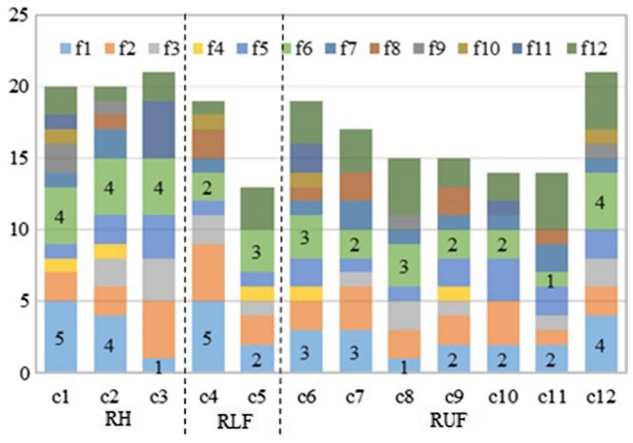

Fig. 7 The number of selections in each feature and channel pair accumulated from ten subjects

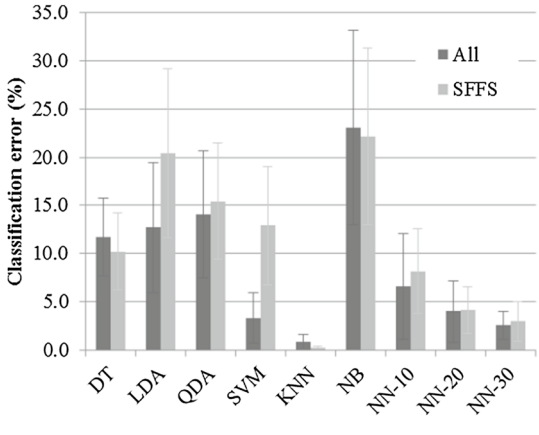

Fig. 8 Classification errors averaged from ten subjects from all feature inputs (dark) compared with those from SFFS feature inputs (gray)

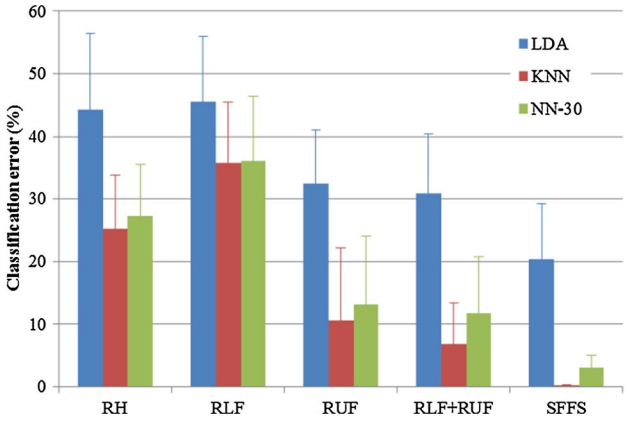

Fig. 9 Classification errors categorized by five muscle regions when the SFFS features are the inputs of the classifiers

Moreover, when considering only a single muscle region, RUF gives better performance than the others.

4 Discussion

Results from SFFS indicate that some features and channels are not necessary for force classification. The features f1, f6, and f12, which are DASDV, MFL, and WL, respectively, are useful for classifying force levels. They would be applied to the real-time EMG recognition system as a single feature. Instead of using RMS [5, 26] or MAV [27], which is used as the single feature in previous studies, the use of one among 3 features, i.e., DASDV, MFL, and WL, may provide better accuracy.

In channel selection, the muscles in RH are more important than other groups because they are directly responsible for thumb-index pinch, especially the AP muscle (c1) [28]. In RLF, the FPL muscle (c4) is more important than the EPL muscle (c5) causing from the adduction effect [28]. Although there is no specific muscle position in RUF, the electrode placements of c9 and c10 could be removed. However, c12 in RUF is the most frequently selected channel. Therefore, it should be included in the prosthetic design applications.

As shown in Fig. 8, when comparing classification errors among 3 muscle regions, namely, RH, RLF, and RUF, results indicate that the muscles in RUF provide lower errors than the muscles in other regions. Although the muscles in RLF were usually found in sEMG classifications of finger movements in previous studies [1, 19, 29, 30], they gave the highest errors in this study. However, when using the muscles in RLF combined with the muscles in RUF, the classification errors slightly decrease. Therefore, the muscles in RLF and RUF are helpful for prosthetic design applications, especially in the wrist disarticulation amputee and the transradial amputee.

Table 3 Example of confusion matrix from the testing data (tenfold cross-validation) in subject 2

	True class				
	10	30	50	70	100
LDA predicted class					
10	551	79	0	0	0
30	58	511	60	1	0
50	1	104	471	54	0
70	0	0	75	542	13
100	0	0	1	80	549
KNN predicted class					
10	630	0	0	0	0
30	0	630	0	0	0
50	0	0	630	0	0
70	0	0	0	629	1
100	0	0	0	0	630
NN-30 predicted class					
10	629	1	0	0	0
30	3	620	7	0	0
50	0	9	610	11	0
70	0	0	11	616	3
100	1	0	0	8	621

To obtain more insight into the accuracy, Table 3 shows the confusion matrix from the testing data classified by LDA, KNN, and NN-30 in subject 2. The feature set selected by SFFS was used as the input of the classifiers. The results indicated that KNN outperformed LDA and NN-30, which agree with the accuracy shown in Figs. 8 and 9.

5 Conclusions

This paper presents the selection of sEMG channels and features for the classification of force levels in a thumb-index pinch. The sEMG data were recorded from 3 muscle regions (12 channels) of 10 non-amputee subjects. Twelve traditional time-domain features were extracted. The SFFS was applied for searching the best subset of channels and features. Each force level signal was trained and classified using 7 classifiers. Results show that KNN and NN can give higher performance than others. The group of muscles and feature set selected by SFFS method can perform to comparable the set of all muscle channels and features. Three features consisting of DASDV, MFL, and WL are primarily selected in the classification. The most frequently selected group of muscles is RH muscle. However, the combination of RLF and RUF can perform high performance, which is

helpful for prosthetic design applications, especially in the wrist disarticulation amputee and transradial amputee.

Many possible directions for future research can be done. For the elimination of power line interference contaminated in the sEMG signal, the edge preserving denoising methods based on variational models [31, 32] may provide better results compared to the standard notch filter. Another direction is the use of a convolutional neural network (CNN). The inherent features generated from the residue muscles using CNN may provide enough accurate force estimation for a control system.

Acknowledgements This work was jointly funded by the Thailand Research Fund and Faculty of Engineering, Prince of Songkla University through Contract No. RSA5980049, in part by the Higher Education Research Promotion and National Research University Project of Thailand, Office of the Higher Education Commission. This research was also supported by the Postdoctoral Fellowship from Prince of Songkla University.

References

1. Resnik, L., Meucci, M.R., Lieberman-Klinger, S., Fantini, C., Kelty, D.L., Disla, R., Sasson, N.: Advanced upper limb prosthetic devices: implications for upper limb prosthetic rehabilitation. Arch. Phys. Med. Rehabil. **93**, 710–717 (2012)
2. Geethanjali, P.: Myoelectric control of prosthetic hands: state-of-the-art review. Med. Devices (Auckl) **9**, 247–255 (2016)
3. Al-Jumaily, A., Olivares, R.A.: Bio-driven system-based virtual reality for prosthetic and rehabilitation systems. Signal Image Video Process. **6**, 71–84 (2012)
4. Kakoty, N.M., Saikia, A., Hazarika, S.M.: Exploring a family of wavelet transforms for EMG-based grasp recognition. Signal Image Video Process. **9**, 553–559 (2015)
5. Kamavuako, E.N., Farina, D., Yoshida, K., Jensen, W.: Relationship between grasping force and features of single-channel intramuscular EMG signals. J. Neurosci. Methods **185**, 143–150 (2009)
6. He, J., Zhang, D., Sheng, X., Li, S., Zhu, X.: Invariant surface EMG feature against varying contraction level for myoelectric control based on muscle coordination. IEEE J. Biomed. Health Inform. **19**(3), 874–882 (2015)
7. Kilic, E.: EMG based neural network and admittance control of an active wrist orthosis. J. Mech. Sci. Technol. **31**(12), 6093–6106 (2017)
8. Al-Timemy, A.H., Khushaba, R.N., Bugmann, G., Escudero, J.: Improving the performance against force variation of EMG controlled multifunctional upper-limb prostheses for transradial amputees. IEEE Trans. Neural Syst. Rehabil. Eng. **24**(6), 650–661 (2016)
9. Celadon, N., Došen, S., Binder, I., Ariano, P., Farina, D.: Proportional estimation of finger movements from high-density surface electromyography. J. Neuroeng. Rehabil. **13**, 73 (2016)
10. Adewuyi, A.A., Hargrove, L.J., Kuiken, T.A.: Evaluating EMG feature and classifier selection for application to partial-hand prosthesis control. Front. Neurorobot. **19**, 10–15 (2016)
11. Theodoridis, S., Koutroumbas, K.: Pattern Recognition. Academic Press, London (2006)
12. Pudil, P., Novovičová, J., Kittler, J.: Floating search methods in feature selection. Pattern Recognit. Lett. **15**(11), 1119–1125 (1994)
13. Thongpanja, S., Phinyomark, A., Quaine, F., Laurillau, Y., Limsakul, C., Phukpattaranont, P.: Probability density functions of stationary surface EMG signals in noisy environments. IEEE Trans. Instrum. Meas. **65**(7), 1547–1557 (2016)
14. Oskoei, M.A., Hu, H.: Myoelectric control systems—a survey. Biomed. Signal Process. Control **2**(4), 275–294 (2007)
15. Arjunan, S.P., Kumar, D.K.: Decoding subtle forearm flexions using fractal features of surface electromyogram from single and multiple sensors. J. Neuroeng. Rehabil. **7**, 53 (2010)
16. Jain, A.K., Duin, R.P.W., Mao, J.: Statistical pattern recognition: a review. IEEE Trans. Pattern Anal. Mach. Intell. **22**, 4–37 (2000)
17. Rokach, L., Maimon, O.: Top-down induction of decision trees classifiers—a survey. IEEE Trans. Syst. Man Cybern. Part C Appl. Rev. **35**(4), 476–487 (2005)
18. Aydemir, O., Kayikcioglu, T.: Investigation of the most appropriate mother wavelet for characterizing imaginary EEG signals used in BCI systems. Turk. J. Electr. Eng. Comput. Sci. **24**, 38–49 (2016)
19. Altin, C., Er, O.: Designing wearable joystick and performance comparison of EMG classification methods for thumb finger gestures of joystick control. Biomed. Res. **28**(11), 4730–4736 (2017)
20. Vapnik, V.N.: Statistical Learning Theory. Wiley, New York (1998)
21. Mccue, R.: A comparison of the accuracy of support vector machine and Naïve Bayes algorithms in spam classification. University of California at Santa Cruz, CA, Nov 2009
22. Scholkopf, B., Sung, K.K., Burges, C.J., Girosi, F., Niyogi, P., Poggio, T., Vapnik, V.: Comparing support vector machines with Gaussian kernels to radial basis function classifiers. IEEE Trans. Signal Process. **45**(11), 2758–2765 (1997)
23. Ding, Y., Pardon, M.C., Agostini, A., Faas, H., Duan, J., Ward, W.O.C., Easton, F., Auer, D., Bai, L.: Novel methods for microglia segmentation, feature extraction and classification. IEEE ACM Trans. Comput. Biol. Bioinform. **14**(6), 1366–1377 (2017)
24. Cover, T., Hart, P.: Nearest neighbor pattern classification. IEEE Trans. Inf. Theory **13**, 21–27 (1967)
25. Borgelt, C., Timm, H., Kruse, R.: Probabilistic networks and fuzzy clustering as generalizations of Naive Bayes classifiers. In: Reusch, B., Temme, Karl-Heinz (eds.) Computational Intelligence in Theory and Practice. Advances in Soft Computing, pp. 121–138. Physica, Heidelberg (2001)
26. Tang, Z., Yu, H., Cang, S.: Impact of load variation on joint angle estimation from surface EMG signals. IEEE Trans. Neural Syst. Rehabil. Eng. **24**(12), 1342–1350 (2016)
27. Choi, C., Kwon, S., Park, W., Lee, H., Kim, J.: Real-time pinch force estimation by surface electromyography using an artificial neural network. Med. Eng. Phys. **32**(5), 429–436 (2010)
28. Lee, S.K., Wisser, J.R.: Restoration of pinch in intrinsic muscles of the hand. Hand Clin. **28**, 45–51 (2012)
29. Riillo, F., Quitadamo, L.R., Cavrinia, F., Gruppioni, E., Pinto, C.A., Pastò, N.C.: Optimization of EMG-based hand gesture recognition: supervised vs. unsupervised data preprocessing on healthy subjects and transradial amputees. Biomed. Signal Process. Control **14**, 117–125 (2014)
30. Malešević, N., Marković, D., Kanitz, G., Controzzi, M., Cipriani, C., Antfolk, C.: Vector autoregressive hierarchical hidden Markov models for extracting finger movements using multichannel surface EMG signals. Complexity **1**, 1–12 (2018)
31. Lu, W., Duan, J., Qiu, Z., Pan, Z., Liu, R.W., Bai, L.: Implementation of high-order variational models made easy for image processing. Math. Methods Appl. Sci. **39**(14), 4208–4233 (2016)
32. Mohan, N., Kumar, S., Poornachandran, P., Soman, K.P.: Modified variational mode decomposition for power line interference removal in ECG signals. Int. J. Electr. Comput. Eng. **6**(1), 151–159 (2016)